North Atlantic Oscillation Index Difference in sea-level atmospheric pressure between Lisbon, Portugal (or Ponta Delgada, Azores) and Reykjavik, Iceland.
Nuclear DNA Genetic material of the nucleus of cells, a component of which is passed to offspring from both female and male parents.
Nucleotide Fundamental structural unit of the nucleic acid group of organic macromolecules, here those involved in information storage (in DNA: units containing adenine, cytosine, guanine or thymine), the sequences of which form codes for protein synthesis.
Otolith Concretions of calcium carbonate in a protein matrix deposited in the inner ears of bony fishes, frequently sectioned to examine annual or daily growth.
Panmixia The characteristic of a species being composed of a single breeding population.
Pelagic Areas of the ocean, or organisms dwelling, well away from the bottom of the sea.
Plankton Organisms in the water column of oceans and lakes that have weak swimming abilities, and are wafted by currents.
Recruitment The entry of organisms, typically fishes, into the next stage of a life cycle or into a fishery by virtue of growth or migration.
Regime shift A transition in oceanic conditions from one quasi-stable state to another.
Selective tidal stream transport Mechanism whereby an organism migrates along the tidal axis by ascending into the water column when the tide is flowing in the appropriate direction and descending to hold position near the bottom when the tide is flowing in the inappropriate direction.
Subtropical gyre Anticyclonic circular pattern of circulation in each of the major ocean basins between the equator and the temperate zone.
Subtropical convergence An area of the ocean where waters of differing characteristics come together, in this case equatorial and temperate waters meeting in the subtropical regions of the Northern and Southern Hemispheres.
Swim-bladder retia Countercurrent network of capillaries on the surface of a fish's swim bladder allowing gas pressure to increase and causing diffusion of gas into the swim bladder.
Western boundary current Western geostrophic currents of subtropical circulation gyres which are swift, deep, and narrow.
Zonal Distribution of oceanic characteristics or organisms on an east–west (latitudinal) axis.

Further Reading

Bruun AF (1963) The breeding of the North Atlantic freshwater-eels. *Advances in Marine Biology* 1: 137–169.
FishBase, A Global Information System on Fishes. http//www.fishbase.org/search.cfm.
Hulet WH and Robins CR (1989) The evolutionary significance of the leptocephalus larva. In: Böhlke EB (ed.) *Fishes of the Western North Atlantic*, part 9, vol. 2, pp. 669–677. New Haven, CT: Sears Foundation for Marine Research, Yale University.
Schmidt J (1922) The breeding places of the eel. *Philosophical Transactions of the Royal Society of London, Series B* 211: 179–210.
Smith DG (1989) Order Anguilliformes, Family Anguillidae, freshwater eels. In: Böhlke EB (ed.) *Fishes of the Western North Atlantic*, part 9, vol. 1, pp. 25–47. New Haven, CT: Sears Foundation for Marine Research, Yale University.
Tesch F-W (1977) *The Eel. Biology and Management of Anguillid Eels*. London: Chapman and Hall.
Tesch F-W (1999) *Der Aal*, 3rd edn. Berlin: Parey. (In German).
Tucker DW (1959) A new solution to the Atlantic eel problem. *Nature* 183: 495–501.
Usui A (1991) *Eel Culture*. Oxford: Fishing News Books.

EKMAN TRANSPORT AND PUMPING

T. K. Chereskin, University of California San Diego, La Jolla, CA, USA
J. F. Price, Woods Hole Oceanographic Institution, Woods Hole, Massachusetts, USA

doi:10.1006/rwos.2001.0155

Introduction

Winds blowing along the ocean's surface exert forces that set the oceans in motion, producing both currents and waves. Separating the wind force into the part that goes into making currents from that which goes into making waves is in fact very difficult. Conceptually, normal forces (i.e., think of the wind beating on the ocean surface like a drum) create waves, and tangential forces (i.e., frictional stresses exerted by the wind pulling on the sea surface) go into making currents. Although there are wind-generated currents that flow in a direction more or less downwind, the currents driven by the steady or slowly varying (compared to the period of the earth's rotation) wind stress flow in a direction

that is quite different from the wind direction, sometimes by more than 90°, due to the combined effects of the wind force and the earth's rotation. These wind-driven currents, commonly called Ekman layer currents in recognition of the Swedish oceanographer W. Ekman who first described their dynamics, are the topic of this article, which has three themes: (1) the local dynamics of Ekman layer currents; (2) the spatial variation of wind stress and the resulting spatial variation of the Ekman layer currents; and (3) the effects of Ekman layer currents on the physical and biological environment of the oceans.

The effects of Ekman layer currents are quite far reaching despite the fact that the currents themselves are usually modest, typically no more than 0.05–0.1 m s^{-1} and smaller than many other currents. The importance of Ekman layer currents arises more from their horizontal spatial extent and variation than from their magnitude alone. Although small in magnitude and in vertical extent (typically the layer extends from the surface to about 100 m depth), the mass transport in the Ekman layer (integrated across the width of the ocean) can be substantial, comparable to the transport of major ocean currents such as the Gulf Stream or the Kuroshio. Spatial variation in the Ekman transport is caused by spatial variation in the wind (the wind stress curl) and results in an exchange of fluid with the ocean interior (Ekman pumping); this exchange of mass induces motion in the ocean interior in order to conserve angular momentum. In regions where the Ekman transport converges, conservation of mass requires that fluid be pumped from the surface Ekman layer into the ocean interior; in regions where the Ekman transport diverges, fluid is pumped into the Ekman layer from below. It is through the vertical velocity or pumping thus generated at the base of the Ekman layer that the wind ultimately forces the ocean interior circulation. Ekman pumping also transports material (nutrients, heat, etc.) from the upper thermocline toward the photic zone and sea surface. The pattern of converging and diverging Ekman layer currents is thus imprinted very strongly upon the patterns of biological productivity as well as upon the strength and shape of the major oceanic current gyres.

Ekman's Theory of the Wind-driven Currents

In 1905 Ekman published a simple but elegant theory to explain F. Nansen's observations of ice movements. Nansen was an oceanographer and Arctic explorer; he observed that wind blowing over ice floes caused them to drift at an angle of 20–40° to the right of the wind rather than downwind, and he correctly surmised that the earth's rotation was causing the ice to move at an angle to the wind. Ekman was the first to derive the equations that describe these surface-layer currents, and he used the solution to explain Nansen's observation.

Ekman assumed that the direct influence of the wind was confined to a surface layer, a frictional boundary layer approximately 10–100 m deep, where a steady wind stress was balanced by the Coriolis force. The Coriolis force is an apparent force due to the earth's rotation; it cannot set the fluid in motion, but it can act to change the motion over timescales of days or longer (i.e., timescales on the order of the earth's rotation period). Ekman's key assumptions were: (1) a steady wind blowing over the ocean surface, far from any coast, (2) a flat ocean surface, (3) a constant water density, and (4) a frictional force acting in the surface boundary layer that matched the wind stress at the sea surface and decayed to zero at the bottom of the surface layer. (An inviscid assumption, i.e., neglect of frictional forces, is valid for most of the ocean except near boundaries.) By making these assumptions Ekman arrived at a greatly simplified theoretical ocean, yet he retained the physics required to explain the wind-driven surface currents. For example, if the sea surface is horizontal and the density is uniform, the pressure at any depth is constant, and there will be no pressure-driven flows. In the real ocean, the tilt of the sea surface and the internal horizontal density gradients result in flows due to the pressure-gradient force, and separating these pressure-driven flows from wind-driven currents is the main challenge in direct testing of Ekman's theory from observations.

The Coriolis force is given by the vector cross-product

$$\text{Coriolis force} = \rho f \hat{\boldsymbol{k}} \times \vec{\boldsymbol{u}}; \quad f = 2\Omega \sin\phi, \qquad [1]$$

where ρ is the density of seawater, $\hat{\boldsymbol{k}}$ is the unit vector in the direction of the local vertical, and $\vec{\boldsymbol{u}} = (u, v)$ is the vector of east (u) and north (v) horizontal currents. The Coriolis parameter f is twice the magnitude of the vertical component of the Earth's rotation vector Ω (2π radians per sidereal day) and ϕ is the latitude. Ekman's steady momentum balance is between the Coriolis force and the vertical gradient of the frictional stress $\vec{\tau} = (\tau^x, \tau^y)$:

$$\rho f \hat{\boldsymbol{k}} \times \vec{\boldsymbol{u}} = \frac{\partial \vec{\tau}}{\partial z} \qquad [2]$$

At the sea surface the frictional stress equals the wind stress $\vec{\tau}_0$. Bulk formulae parameterize the wind stress in terms of a wind velocity at 10 m above the sea surface $\vec{U}_{10}$, the air density ρ_{air}, and a drag coefficient C_D:

$$\vec{\tau}_0 = \rho_{\text{air}} C_D \vec{U}_{10} |\vec{U}_{10}| \quad [3]$$

A wind speed of $10\,\text{m s}^{-1}$ corresponds to a stress of about $0.1\,\text{N m}^{-2}$.

Ekman's assumption that the frictional force acted only in the surface layer allowed him to estimate the volume transport within the layer by integrating from the sea surface, where the wind stress was known, to the unknown depth $-H$ where the frictional stress vanished by assumption. The Ekman transport relation is given by

$$M_x = \frac{\tau_0^y}{\rho f}; \quad M_y = -\frac{\tau_0^x}{\rho f} \quad [4]$$

where M_x is the eastward component of Ekman transport and M_y is the northward component. One of the surprising results of the theory is that the net transport is at right angles to the wind direction and depends only on the wind stress at the sea surface. Most notably, the transport does not depend on the details of how the stress gets transferred through the Ekman layer. The northward wind component τ_0^y forces the eastward Ekman transport M_x, and the eastward wind component τ_0^x forces the northward Ekman transport M_y. The sign (to the right/left) of the wind depends on the sign of the Coriolis parameter f, which is positive/negative in the Northern/Southern Hemisphere, respectively. The transport is in units of $\text{m}^2\,\text{s}^{-1}$, and it can be interpreted as the rate at which the volume (per unit width) of water in the Ekman layer is moving. The qualifier 'per unit width' emphasizes that this is the transport at a single point location; in practice, one is usually interested in integrating the Ekman transport over some distance, such as a latitude or longitude band, to see the total volume of water in the Ekman layer that is transported across that latitude or longitude.

Spatial variation in the wind and therefore in the Ekman transport results in local convergences and divergences within the surface layer. The vertical velocity (Ekman pumping) w_H that results from convergence or divergence in the Ekman layer is derived by integrating the mass conservation equation over the Ekman layer:

$$w_H = \frac{\partial(\tau_0^y/\rho f)}{\partial x} - \frac{\partial(\tau_0^x/\rho f)}{\partial y} \quad [5]$$

Thus the Ekman pumping is given by the spatial derivative or curl of the wind stress (divided by ρf); it depends on the spatial variation of the wind rather than its magnitude.

Ekman's theory also predicted the currents within the surface layer. His solution for the velocity structure, the Ekman spiral, is the least robust of his results since it depends critically on how one assumes the stress that the wind exerts on the surface is transferred downward by friction and mixing. Ekman was the first to acknowledge that the wind momentum is transferred to ocean currents through turbulent mixing. He modeled it as a diffusion process, exactly analogous to molecular diffusion, but with an effective kinematic viscosity (eddy viscosity) many orders of magnitude larger than molecular viscosity. Turbulent eddies are much more efficient than molecular diffusion at stirring the fluid and hence mixing the wind momentum. For example, a wind of $10\,\text{m s}^{-1}$ would require more than a day to penetrate the top meter of the surface layer if molecular diffusion were the sole process acting to mix the wind momentum. In fact, the wind momentum is observed to mix down by tens of meters within hours. Although turbulence is clearly the dominant process in creating the wind-mixed layer, the detailed structure of the turbulent boundary layer remains an active research question today (*see* **Upper Ocean Mixing Processes**).

To solve for the currents, Ekman assumed a constant eddy viscosity A_v in place of the molecular viscosity ν. The value of ν for sea water is approximately $10^{-6}\,\text{m}^2\,\text{s}^{-1}$ and applies for smooth laminar flow. The magnitude and structure of a turbulent eddy viscosity A_v are not well known, but scaling arguments suggest that its magnitude may be as large as $10^{-1}\,\text{m}^2\,\text{s}^{-1}$. The current structure is a spiral (**Figure 1**) that decays in amplitude and rotates clockwise with increasing depth (z negative):

$$u = \exp(z/D_E)[V_+ \cos(z/D_E) + V_- \sin(z/D_E)]$$

$$v = \exp(z/D_E)[V_+ \sin(z/D_E) - V_- \cos(z/D_E)] \quad [6]$$

$$V_+ = \frac{\tau_0^x + \tau_0^y}{\rho\sqrt{(2A_v|f|)}}; \quad V_- = \frac{\tau_0^x - \tau_0^y}{\rho\sqrt{(2A_v|f|)}}$$

The Ekman depth, $D_E = \sqrt{(2A_v/|f|)}$, is the depth over which the amplitude decays by 1/e and over which the velocity vector rotates by one radian. Note that the predicted surface current lies at an angle of 45° to the wind direction.

Ekman spirals have been observed in the laboratory, where the appropriate viscosity is the molecular

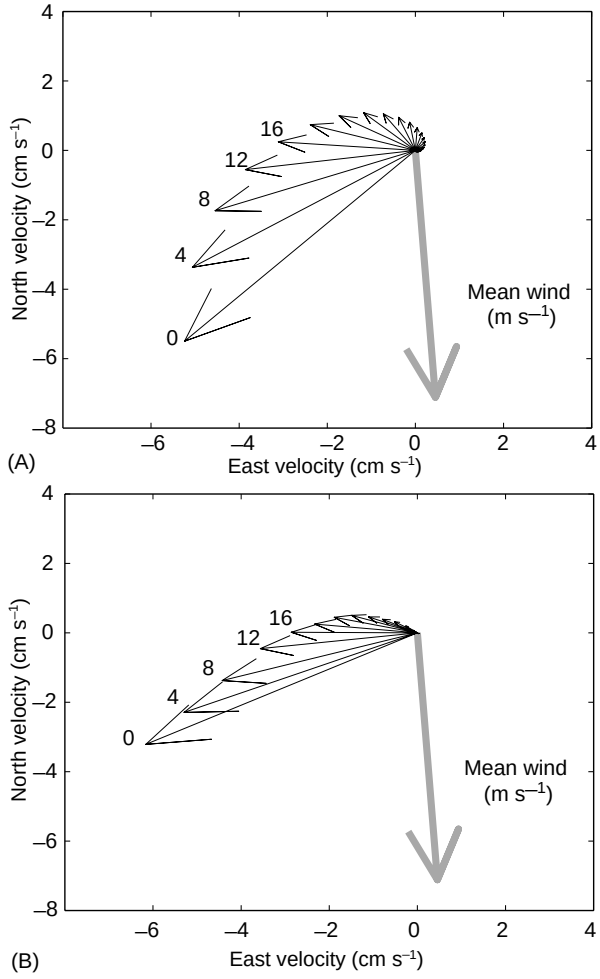

Figure 1 Comparison of an observed wind-forced velocity spiral and the theoretical Ekman spiral calculated for the same wind in the Northern Hemisphere. Each current vector is the time-averaged velocity at a particular depth; the first five depths are labelled. Depth units are m, current velocity units are cm s^{-1}, and wind velocity units are $m\,s^{-1}$. (A) The theoretical Ekman spiral: the surface current lies 45° to the right of the wind, and the rate of amplitude decay and the rate of rotation with depth are both set by the constant eddy viscosity ($0.014\,m^2\,s^{-1}$), chosen to match the rate of amplitude decay of the observed spiral. (B) Observed velocity spiral from averaged current observations from a location about 400 km offshore of the US west coast from the Eastern Boundary Currents Experiment. The currents spiral to the right of the wind direction and decay with depth, as predicted by the theory. However, the surface current lies more than the predicted 45° to the right of the wind, and the current amplitude decreases at a faster rate than it turns to the right, resulting in a flatter spiral than the theory predicts. These differences are due to unmodeled processes.

value v. More limited observations are available in the open ocean, because of the difficulty in acquiring observations with the requisite vertical resolution and because of the difficulty in separating the wind-driven flow from pressure-driven flow. Ocean spirals have been observed (**Figure 1**); they tend to be flatter than Ekman's theory predicts, due to the effect of other processes such as stratification and the diurnal cycling of the mixed layer depth. Regardless of these details, integrating the Ekman spiral (eqn [6]) over the surface layer yields the more general Ekman transport result (eqn [4]).

Ekman Transport and Pumping

One of the remarkable results of Ekman's theory is the Ekman transport relation (eqn [4]), which allows the surface layer transports to be predicted from the wind field. Ship observations of wind have been made over a much longer period of time and over a much greater area of the ocean than have direct measurements of ocean currents, and satellites presently provide global coverage of the wind field. Wind velocity is the quantity that is typically measured, at heights from 10 to 30 m above the sea surface. Wind stress is proportional to the wind speed squared and in the same direction as the wind velocity.

A first step in calculating wind stress from velocity measurements is to determine the wind speed at 10 m height above the sea surface, using a model of the wind profile versus height. The stress at the sea surface can then be calculated using eqn [3] that parameterizes the stress using the 10-m wind speed and a drag coefficient that depends on the speed and other properties of the air–sea interface such as air and sea temperature and relative humidity. Direct estimation of the wind stress requires measuring the turbulent eddies in the atmospheric boundary layer above the sea surface. These measurements are more difficult to make and hence are not made routinely; however, they are critical to improving and validating the bulk formulae.

The Ekman transport relation predicts a transport at right angles to the wind stress, in direct proportion to the wind and inversely proportional to the Coriolis parameter. The theory cannot be applied at the equator where $f = 0$. For a wind stress of $0.1\,N\,m^{-2}$, and a seawater density of about $1025\,kg\,m^{-3}$, the transport per unit width at a latitude of 30° is $1.3\,m^2\,s^{-1}$ and at a latitude of 10° it is $3.4\,m^2\,s^{-1}$. Integrated across an ocean basin, the Ekman transport can be quite large. The Atlantic Ocean at 10°N is about 4000 km across. The mean wind stress is of order $0.1\,N\,m^{-2}$, and the predicted Ekman transport is $15 \times 10^6\,m^3\,s^{-1}$. This transport is about one-half the transport measured for the Gulf Stream where it passes through the Straits of Florida. Across the same latitude in the Pacific, the Ekman transport is estimated to be about

$50 \times 10^6\,\mathrm{m^3\,s^{-1}}$, not because the winds are stronger but because the Pacific is about three times the width of the Atlantic at that latitude.

The wind stress is communicated to the ocean interior through Ekman pumping, and therefore the spatial variation of the Ekman transport is just as important as its magnitude. The large-scale pattern of the wind is one of alternating bands of easterlies and westerlies (**Figure 2A**). The equator is spanned by a broad band of easterly winds known as the trade winds. The magnitude of these winds decreases with latitude, reaching a minimum about 30° or so away from the equator. Still further north/south lies the band known as the prevailing westerlies, with a maximum at about 50° latitude. The polar easterlies are the most poleward band of winds. This overall pattern dominates in both hemispheres of the Pacific and Atlantic Oceans. The Ekman transport relation implies a corresponding pattern of convergences and divergences in the Ekman transport that should be detectable through the Ekman pumping of ocean current gyres (**Figure 2C**). For example, the theory suggests that the persistent easterly trade winds in the tropics will force a poleward Ekman transport; the midlatitude westerlies will force an equatorward Ekman transport. The resulting Ekman transport convergence at subtropical latitudes should result in a thick warm layer of water above the main thermocline, an Ekman pumping that supplies fluid to the ocean interior, and, through conservation of angular momentum, a clockwise/anticlockwise general circulation in the northern/southern hemisphere. Such gyres are major observed features of the subtropical oceans. Their existence is an indirect confirmation of Ekman's theory. It is through the pumping thus generated at the base of the Ekman layer that the wind ultimately forces the ocean interior. If the wind were spatially uniform, the wind-driven currents and mass transport would remain largely confined within the shallow surface Ekman layer and would have a negligible role in driving ocean circulation.

Note that using the wind to estimate the Ekman transport via eqn [4] gives no indication of how deep it extends. Direct verification, from measurements of both wind and currents, is required in order to determine the details of the turbulent mixing of the wind momentum, such as the maximum depth of frictional influence of the wind, and the importance of other processes such as time dependence and stratification. This direct confirmation eluded oceanographers until quite recently, because of the difficulty in making accurate measurements in the harsh surface zone and in separating the

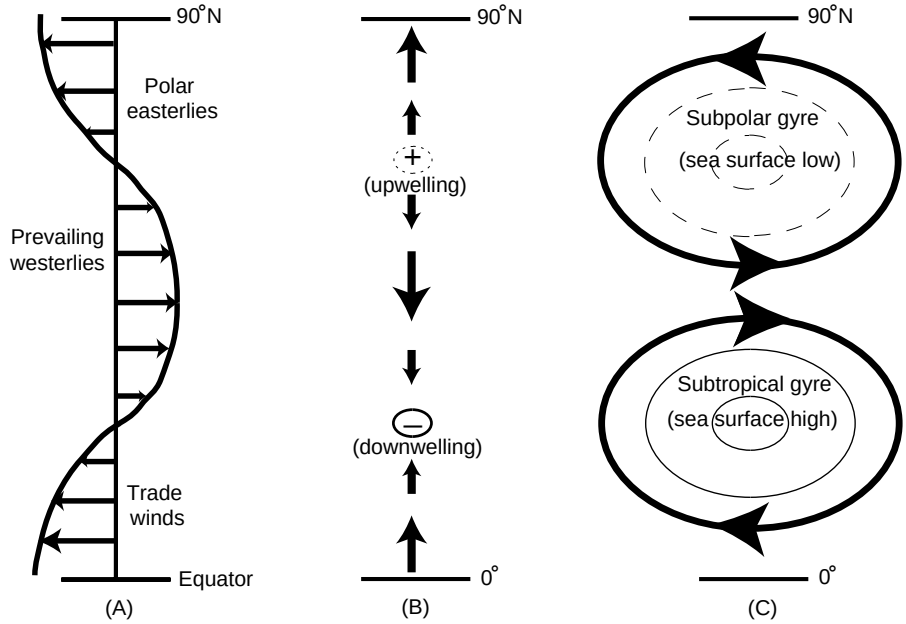

Figure 2 Schematic of the relation between zonal wind stress, Ekman transport and pumping, and ocean current gyres. (A) Zonal wind stress for the Northern Hemisphere, with easterly wind stress near the equator and the pole, and westerly wind stress at midlatitudes. (B) The meridional Ekman transport that results from the zonal wind stress. The magnitude is proportional to the wind stress, and the direction is orthogonal to the wind direction. The spatial variation in the wind stress results in Ekman convergences and divergences and Ekman pumping. (C) The wind-driven oceanic current gyres. Ekman convergence in the subtropics results in a sea-surface high and a clockwise-current gyre with downwelling at the gyre center. The Ekman divergence at subpolar latitudes results in a sea-surface low and an anticlockwise-current gyre with upwelling at the gyre center.

wind-driven flow from other pressure-driven flows. Also, since the wind is not steady, appropriate timescales for averaging need to be determined. Direct verification of the integrated Ekman transport has been made from measurements at tropical latitudes 8–11°N in the Atlantic, Pacific, and Indian Oceans, where the Ekman transport is large. High vertical resolution moored measurements at midlatitudes in the Atlantic and the Pacific have verified the Ekman transport relation for moderate winds, with transport per unit width of about $1\,m^2\,s^{-1}$.

Ekman transport and pumping have far-reaching implications, from the mechanism of momentum transfer from wind to water to the maintenance of the large-scale wind-driven oceanic current gyres. Although the original theory was developed for a steady wind, the phenomena of Ekman transport and pumping occur on much shorter timescales, e.g., the scale of synoptic storms. However, Ekman transport and pumping are most effective in driving large-scale ocean circulation when the wind is steady over long periods of time, because then the effects can accumulate.

Coastal Upwelling

Although spatial variation in the wind field is the cause of Ekman pumping in the open ocean, a spatially uniform wind blowing parallel to a coast can also cause Ekman pumping. In the Northern Hemisphere, Ekman divergence occurs when the wind blows parallel to a coastline on its left. For example, during spring and summer the mean winds along the west coast of North America are southward. Associated with these winds is a net westward Ekman transport. This offshore transport of mass in the surface layer is balanced by an onshore flow at depth and an Ekman pumping of water from depth into the surface layer (**Figure 3**). This phenomenon is known as coastal upwelling, and it occurs seasonally along the west coasts of continents in both hemispheres. Prolonged upwelling can provide a continuous source of cold, nutrient-rich water to the surface layer euphotic zone, replacing the nutrient-depleted water that is transported offshore. Many of the ocean's important fisheries are concentrated in upwelling zones. The reverse phenomenon, convergence from onshore Ekman transport and downward pumping at the coast also occurs and is called downwelling.

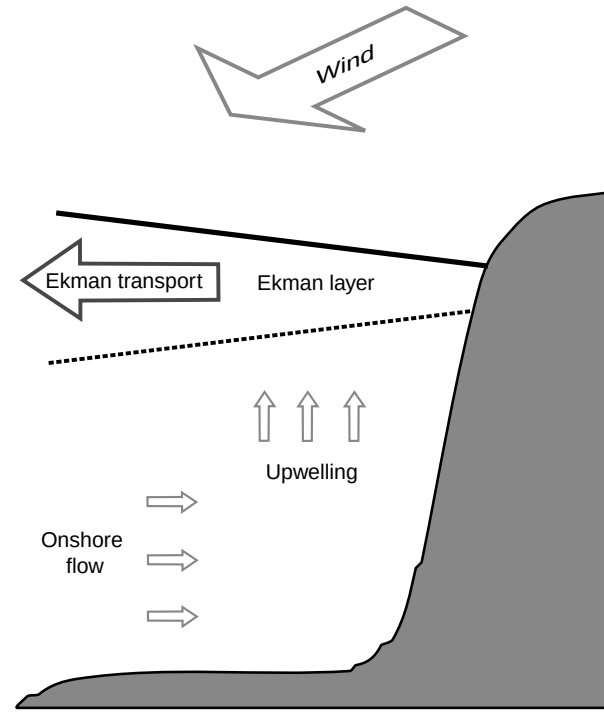

Figure 3 Diagram of upwelling (Ekman divergence) at a coast. The wind blows parallel to the coast (in a direction *out* of the diagram in the Northern Hemisphere), forcing a net Ekman transport offshore. This offshore transport is compensated by onshore flow at depth and upwelling.

Summary

Ekman's theory of wind-driven currents, now almost 100 years old, is a cornerstone of physical oceanography. The two essential features of the theory – that the dominant momentum balance for steady wind-driven currents is between the wind stress and Coriolis acceleration and that wind stress is transmitted through the upper ocean as a turbulent momentum flux – are now well established by observation. The most important predictions of the theory, the transport relation and Ekman pumping, form the essential link between the winds and our understanding of the wind-driven ocean circulation and is also established by observation. Yet there are other aspects of Ekman's theory, most notably the eddy diffusivity, that are still unsettled in the sense that they cannot be derived strictly from a more general theory, and neither is there strong support for eddy diffusivity from observation. This may seem to indicate unusually slow progress on this important point, and yet the uncertainty surrounding eddy diffusivity is no more than a reflection of the tortuous development of turbulent transfer theory generally. It seems likely that succeeding editions of this encyclopedia will relate a similar story on this point, at least.

See also

Internal Tidal Mixing. Meddies and Sub-surface Eddies. Mesoscale Eddies. Seabird Population

Dynamics. Upper Ocean Mixing Processes. Wave Generation by Wind. Wind and Buoyancy-forced Upper Ocean. Wind Driven Circulation.

Further Reading

Chereskin TK (1995) Direct evidence for an Ekman balance in the California Current. *Journal of Geophysical Research* 100: 18261–18269.

Ekman VW (1905) On the influence of the earth's rotation on ocean-currents. *Arkiv för Matematik, Astronomi och Fysik* 2: 1–52.

Gill AE (1982) *Atmosphere–Ocean Dynamics*. New York: Academic Press.

Pond S and Pickard GL (1983) *Introductory Dynamical Oceanography*, 2nd edn. Oxford: Pergamon.

Price JF, Weller RA and Schudlich RR (1987) Wind-driven currents and Ekman transport. *Science* 238: 1534–1538.

EL NIÑO SOUTHERN OSCILLATION (ENSO)

K. E. Trenberth, National Center for Atmospheric Research, Boulder, CO, USA

doi:10.1006/rwos.2001.0262

Introduction

A major El Niño began in April of 1997 and continued until May 1998. It has been labeled by some as the 'El Niño of the century' as it was certainly the biggest on record by several measures. It brought with it many weather extremes and unusual weather patterns around the world. Moreover, the event was predicted by climate scientists and received unprecedented news coverage, so that the term 'El Niño' became part of the popular vernacular. Many things were blamed on El Niño, and some of them indeed were influenced by El Niño, although in some instances, the connection was, at best, tenuous. Although El Niño may be relatively new to the public, it has been known to scientists, at least in some respects, for decades and even centuries. El Niño refers to the exceptionally warm sea temperatures in the tropical Pacific, but it is linked to major changes in the atmosphere through the phenomenon known as the Southern Oscillation (SO), in particular, so that the whole phenomenon is called El Niño–Southern Oscillation (ENSO) by scientists. This article outlines the current understanding of ENSO and the physical connections between the tropical Pacific and the rest of the world.

ENSO Events

El Niños are not uncommon. Every three to seven years or so, a pronounced warming occurs of the surface waters of the tropical Pacific Ocean. The warmings take place from the International Dateline to the west coast of South America and result in changes in the local and regional ecology, and are clearly linked with anomalous global climate patterns. In 1997, the warming can be seen by comparing the sea surface temperatures (SSTs) in December 1997 at the peak of the 1997/98 event with those a year earlier (**Figure 1**). As well as the total SST fields, this figure also displays the departures from average.

The warmings have come to be known as 'El Niño events'. Historically, 'El Niño' referred to the appearance of unusually warm water off the coast of Peru, where it was readily observed as an enhancement of the normal warming about Christmas (hence Niño, Spanish for 'the boy Christ-child') and only more recently has the term come to be regarded as synonymous with the basinwide phenomenon. The oceanic and atmospheric conditions in the tropical Pacific are seldom close to average, but instead fluctuate somewhat irregularly between the warm El Niño phase of ENSO, and the cold phase of ENSO consisting of basinwide cooling of the tropical Pacific, dubbed 'La Niña events' ('La Niña' is 'the girl' in Spanish). The most intense phase of each event typically lasts about a year.

The SO is principally a global-scale seesaw in atmospheric sea level pressure involving exchanges of air between eastern and western hemispheres (**Figure 2**) centered in tropical and subtropical latitudes with centers of action located over Indonesia and the tropical South Pacific Ocean (near Tahiti). Thus the nature of the SO can be seen from the inverse variations in pressure anomalies (departures from average) at Darwin (12.4°S 130.9°E) in northern Australia and Tahiti (17.5°S 149.6°W) in the South Pacific Ocean (**Figure 3**) whose annual mean pressures are strongly and significantly oppositely correlated. Consequently, the difference in pressure anomalies, Tahiti–Darwin, is often used as a Southern Oscillation Index (SOI). The sequences of swings in the SOI shown in **Figure 3** are discussed below in conjunction with those of SST.

Higher than normal pressures are characteristic of more settled and fine weather, with less rainfall,